The Incredible Lightness of Water Vapor

Da Yang* and Seth Seidel

University of California, Davis

Lawrence Berkeley National Laboratory, Berkeley

Corresponding author address: Da Yang, 253 Hoagland Hall, Davis, CA 95616.

E-mail: dayang@ucdavis.edu

ABSTRACT

The molar mass of water vapor is significantly less than that of dry air. This makes a moist parcel lighter than a dry parcel of the same temperature and pressure. This effect is referred to as the vapor buoyancy effect and has often been overlooked in climate studies. We propose that this effect increases Earth's outgoing longwave radiation (OLR) and stabilizes Earth's climate. We illustrate this mechanism in an idealized tropical atmosphere, where there is no horizontal buoyancy gradient in the free troposphere. To maintain the uniform buoyancy distribution, temperature increases toward dry atmosphere columns to compensate reduction of vapor buoyancy. The temperature difference between moist and dry columns would increase with climate warming due to increasing atmospheric water vapor, leading to enhanced OLR and thereby stabilizing Earth's climate. We estimate that this feedback strength is about $O(0.2\ \mathrm{W/m^2/K})$, which compares with cloud feedbacks and surface albedo feedbacks in current climate.

1. Introduction

How fast would Earth's climate respond to increasing CO_2 (Manabe and Wetherald 1975; Flato et al. 2013; Collins et al. 2013)? Why is tropical climate more stable than extratropical climate (Holland and Bitz 2003; Polyakov et al. 2002; Pierrehumbert 1995)? What sets the inner edge of the habitable zone of Earth-like planets (Yang and Abbot 2014; Pierrehumbert 2010)? Understanding and accurately estimating climate feedbacks are key to address these pressing questions.

The importance of water vapor seems to be widely recognized in the literature of climate feedbacks (Manabe and Wetherald 1967; Ingersoll 1969; Held and Soden 2000; Flato et al. 2013). Previous studies have focused on three basic effects of water vapor: E1) water vapor is a greenhouse gas; E2) water vapor can condense to liquid water and release latent heat; E3) saturation vapor pressure increases with temperature exponentially. The combination of E1 and E3 gives rise to the water vapor feedback, the dominant positive climate feedback (Manabe and Wetherald 1967; Held and Soden 2000; Flato et al. 2013). Increasing temperature leads to more water vapor, which leads to an enhanced greenhouse effect, warming the planet further. The water vapor feedback could even lead to a runaway greenhouse state when the atmosphere is sufficiently opaque to longwave radiation that the outgoing longwave radiation (OLR) is insensitive to surface temperature (Ingersoll 1969). The combination of E2 and E3 gives rise to the (tropical) lapse rate feedback, a negative climate feedback in the tropical atmosphere (Flato et al. 2013). Increasing temperature leads to more water vapor, which leads to less steep lapse rate in the tropical atmosphere. This effect increases upper troposphere temperature more than the lower troposphere, leading to higher emission of outgoing longwave radiation (OLR), which cools the planet. At higher latitudes, temperature lapse rate is no longer controlled by moist convection, so the lapse rate feedback is less constrained. Both feedbacks are among the five most important climate feedbacks in the Intergov-

ernmental Panel on Climate Change (IPCC) reports and have been extensively evaluated in general circulation models (GCMs) (Flato et al. 2013).

However, the lightness of water vapor has been completely overlooked in the context of climate feedbacks. The molar mass of water vapor is 18 g/mol, significantly lighter than that of dry air, which is 29 g/mol. This makes a moist parcel lighter than a dry parcel of the same temperature and pressure (Emanuel 1994). Here we refer to this as the vapor buoyancy effect, though it is also referred to as the virtual effect (Yang 2018a,b).

We propose that the vapor buoyancy effect can increase Earth's OLR and helps stabilize Earth's climate by regulating the atmosphere's thermal structure. Figure 1 shows temperature and virtual temperature (buoyancy) fields in the moisture space from 2^oS to 2^oN using NASA AIRS data. In the free troposphere ($p < 850$ hPa), buoyancy is horizontally uniform because of the small Coriolis parameter and efficient gravity waves (Charney 1963; Bretherton and Smolarkiewicz 1989; Sobel et al. 2001; Yang 2018a). However, temperature increases toward dry columns due to the vapor buoyancy effect. Moving toward the dry columns, moisture and its associated vapor buoyancy are reduced. To maintain uniform buoyancy, temperature has to increase. We propose that the temperature tilt would increase with climate warming due to increasing atmospheric moisture, leading to enhanced OLR over the dry area. This is a negative feedback and can stabilize Earth's climate.

Previous studies have noticed that vapor buoyancy could make temperature increase toward dry columns in the tropical atmosphere (Tompkins 2001; Bretherton and Smolarkiewicz 1989; Bretherton et al. 2005; Yang 2018b,a). However, they have often considered this effect to be small and negligible, simplifying the dynamics according to a weak temperature gradient approximation (Sobel et al. 2001). These studies, therefore, did not consider that its radiative effect is significant, which is the novelty of this study.

In Section 2, we explain our hypothesis in detail. We first illustrate how the vapor buoyancy effect increases Earth's OLR (a negative radiative effect) and then explain why this effect strengthens with climate warming. In Section 3, we derive a simple model for the radiative effect and feedback strength of the vapor buoyancy effect. We then use the simple model to make order-of-magnitude estimates for the radiative effect and feedback strength. In Section 4, we conclude and discuss implications on the climate stability of Earth and other planets.

2. Hypothesis

We propose that the vapor buoyancy can increase OLR (a negative radiative effect) due to a clear-sky effect, and that the radaitive effect increases with climate warming. Figure 2 illustrates our hypothesis by comparing OLR from two stand-alone atmospheres with overturning circulations: one considers the vapor buoyancy effect (control), the other does not consider this effect. The overturning circulation is analogous to the Walker Circulation or convective self-aggregation in the tropics (Bretherton et al. 2005; Pritchard and Yang 2016; Yang and Ingersoll 2013, 2014). The upwelling branch of the circulation is associated with deep convection and moist air, and the downwelling branch is associated with clear sky and dry air. For illustrative purposes, we make a few simplifications: S1) the two atmospheres are non-rotating; S2) the two atmospheres sit above ocean surface with the same, uniform surface temperature; S3) the two atmospheres have the same water vapor distribution. The first two simplifications are relevant to the tropical atmosphere as the rotation effect and surface temperature gradient are both weak in the tropics. The third simplification is often required when calculating the radiative effect.

Figure 2 shows that the control atmosphere emits more OLR than the no-vapor-buoyancy atmosphere due to higher temperature in the dry area. OLR is primarily a function of temperature and water vapor mixing ratio r. When r remains the same in the two atmospheres (S3), the OLR dif-

ference would come from temperature differences between the two atmospheres. The temperature profiles of moist areas in the two atmospheres are set by convective plumes. Because these convective plumes rise from the same surface temperature, the temperature profiles should be almost identical in the two moist areas. Temperature profiles in the dry areas, however, differ significantly, leading to differences in OLR. According to long-accepted results in geophysical fluid dynamics, the horizontal buoyancy gradient is negligible in the free troposphere without rotation because gravity waves can effectively smooth out buoyancy anomalies (Charney 1963; Sobel et al. 2001). We refer to this effect as the weak buoyancy gradient (WBG) approximation (Yang 2018a). In the control atmosphere, buoyancy is a function of both temperature and and water vapor mixing ratio r due to the vapor buoyancy effect. The horizontal moisture gradient then leads to horizontal temperature gradient: dry air is warmer than moist air. In the no-vapor-buoyancy atmosphere, temperature is uniformly distributed in the free troposphere, as buoyancy is a function of temperature only. The dry column of the control atmosphere, therefore, is warmer than that of the no-vapor-buoyancy atmosphere, leading to enhanced OLR.

In warmer climates, the vapor buoyancy effect would become more significant due to increasing water vapor. Therefore, we expect that the radiative effect due to the vapor buoyancy also increases with climate warming. This is a negative climate feedback (Fig. 2b). The proposed mechanism relies on ample atmospheric water vapor, so it would be most effective in stabilizing the tropical climate.

We will construct a simple model of the proposed feedback mechanism. This will give an order-of-magnitude estimate of the associated radiative effect and the rate at which it increases with climate warming.

3. A simple model

We construct a simple model based on the schematic diagram (Fig. 2). Each atmosphere with overturning circulations is represented by a dry column and a moist column (Pierrehumbert 1995). Because the moist columns would have the same temperature profiles, the OLR difference primarily comes from the dry columns, which we will focus on. Again, we aim to estimate the "radiative effect" due to the vapor buoyancy effect. Therefore, we assume that all basic dynamic (*e.g.*, circulation and pressure) and thermodynamic features (*e.g.*, moisture) are the same in the two atmospheres–one with the vapor buoyancy effect, and the other without it.

The goal of this simple model is to provide an order-of-magnitude understanding of our hypothesis. Therefore, we employ a two-band radiative transfer model. The two-band model is more realistic than a gray atmosphere model by allowing two absorption bands with distinct absorption coefficients, leading to different emission levels. The two band model is, on the other hand, much simpler than a real-gas radiative transfer model, so the results are easier to interpret.

a. The two-band model

We consider a plane-parallel atmosphere. Only the clear-sky longwave (IR) radiation is considered, and the IR opacity is mainly due to water vapor. Here we parameterize the water vapor absorption spectrum by two broad bands that occupy roughly equal fractions of blackbody emission at Earth-like temperatures (Beucler and Cronin 2016): one with a strong absorption coefficient (k_S) and the other with a weak absorption coefficient (k_W).

We first consider one absorption band with any given k. OLR is defined as

$$OLR^k \equiv F^{\uparrow}(p = 0) - F^{\downarrow}(p = 0); \tag{1}$$

where $F^{\uparrow}$ and $F^{\downarrow}$ are upward and downward longwave radiative fluxes. We know that $F^{\downarrow}(0) \approx 0$, so a primary focus is to solve for $F^{\uparrow}(0)$ in the gray atmosphere, which is given by

$$\frac{dF^{\uparrow}}{dt} = F^{\uparrow} - \sigma T^4; \tag{2}$$

where T is temperature, t is optical depth, and σ is the Stefan-Boltzmann constant. We integrate (2) and get

$$F^{\uparrow}(0) = e^{-t_s} F^{\uparrow}(t_s) + \int_0^{t_s} \sigma T^4 \times e^{-t'} dt'. \tag{3}$$

The OLR is then given by

$$OLR^k = e^{-t_s} \sigma T_s^4 + \int_0^{t_s} \sigma T^4 \times e^{-t'} dt'; \tag{4}$$

where A_s represents the surface value of A, and we have used $F^{\uparrow}(t_s) = \sigma T_s^4$. This equation shows that *OLR* has two components: one is the surface contribution, and the other is the atmosphere contribution.

We now use (4) to calculte the OLR difference between the two atmospheres, each containing one moist and one dry columns. We remind the readers that T_s, r and thereby t of the two atmospheres are identical, so the OLR difference primarily comes from dry columns, in which there is significant air temperature difference. The OLR difference of the dry column is given by

$$\Delta OLR^k \equiv OLR_v^k - OLR_{nv}^k \approx \int_0^{t_s} 4\sigma T_d^3 \Delta T \times e^{-t'} dt' \approx \int_0^{t_s} 4\sigma T_m^3 \Delta T \times e^{-t'} dt'; \tag{5}$$

where OLR_v and OLR_{nv} represent OLR in the atmosphere with and without the vapor buoyancy effect. In the last equal sign, we assumed that $(T_d - T_m)/T_m \ll 1$. Because the strong and weak absorption bands occupy equal portions of the spectrum, the total OLR difference is given by

$$\Delta OLR = 0.5 \times (\Delta OLR^{k_S} + \Delta OLR^{k_W}). \tag{6}$$

To compute ΔOLR, we need information of T_m, ΔT, t, and thereby r, which is the mixing ratio of water vapor.

b. Temperature

In the Earth's tropical atmosphere, temperature profiles can be approximated by power-law relations of pressure:

$$T = T_s \left(\frac{p}{p_s}\right)^{R_d \Gamma_M / g}; \tag{7}$$

where T_s is the surface temperature, p_s is surface pressure, R_d is the gas constant for dry air, Γ_M is the moist adiabatic lapse rate, and g is gravity acceleration. This has been referred to as the "all-troposphere model" by Pierrehumbert (2010), as the lapse rate is entirely determined by moist convection. Equation (7) fits the observed temperature profiles in the tropical troposphere, but introduces significant biases in the stratosphere (Beucler and Cronin 2016). Earth's OLR is dominated by tropospheric contributions, which justifies the use of (7).

c. Moisture

The water vapor mixing ratio r is the ratio of the mass of water vapor to the mass of dry air and is given by

$$r = RH \times r^*(T; p); \tag{8}$$

where RH is the relative humidity, and r^* is the saturation mixing ratio. For the moist column, we assume that $r_m = r_m^*$ ($RH = 1$) at all vertical levels; For the dry column, we have $r = b \cdot r_m^*$, where $0 < b < 1$. Here b is a more convenient parameter than the relative humidity of dry columns (RH_d). This is because, at given T_s, the two dry columns are of different temperatures, so they would have different RH values corresponding to same mixing ratio. In reality, b could have complicated vertical structures, which requires multiple parameters to describe. For the purpose of illustrating the proposed mechanism with minimal parameters, we take b as a constant at all vertical levels. This simplification may affect the results quantitatively but will not affect the results qualitatively.

d. Optical depth

Outgoing longwave radiation is observed from space, so it would be convenient to define the optical depth t as an increasing function as pressure. We thus require that $t(p = 0) = 0$. We write the optical depth as

$$dt = k \cdot r \cdot \frac{dp}{g}: \tag{9}$$

The optical depth would have different values for the two absorption bands: $dt = k^s \cdot r \cdot dp/g$ for the strong band, and $dt = k^w \cdot r \cdot dp/g$ for the weak band. In this model, we ignore the pressure-broadening effect and treat the absorption coefficients as constant: $k^s = 1.66 \times 0.1$ (m^2/kg) and $k^w = 1.66 \times 0.02$ (m^2/kg), where the factor of 1.66 is referred to as the diffusivity factor (Pierrehumbert 2010). Here the absorption coefficients are consistent with previous modeling studies of similiar complexity (Ingersoll 1969; Pierrehumbert 2010; Beucler and Cronin 2016). We can integrate (9) to obtain the optical depth at an arbitrary pressure level

$$t(p) = \int_0^p k \cdot r \cdot \frac{dp'}{g}: \tag{10}$$

At surface $p = p_s$, we then have $t_s = \int_0^{p_s} k \cdot r \cdot dp'/g$.

e. The WBG approximation and ΔT

Buoyancy is horizontally homogenized in the tropical free troposphere (Fig. 1). We refer to this constraint as the weak buoyancy gradient (WBG) approximation (Yang 2018a). This is an improvement of the weak temperature gradient (WTG) approximation, which neglects the vapor buoyancy effect (Charney 1963; Sobel et al. 2001). In a moist atmosphere, buoyancy is related to the virtual temperature, which is given by

$$T_v = T \quad \frac{1 + r/\epsilon}{1 + r} \quad ; \tag{11}$$

where $\epsilon = M_v/M_d$, where M_v and M_d represent the molar mass of water vapor and dry air, respectively. In the free troposphere, uniform buoyancy requires the virtual temperature to be uniform across the moist and dry area:

$$T_m \left(\frac{1 + r_m/\epsilon}{1 + r_m} \right) = T_d \left(\frac{1 + r_d/\epsilon}{1 + r_d} \right) : \tag{12}$$

We substitute $T_d = T_m + \Delta T_{WBG}$ into (12) and get

$$\Delta T_{WBG} = T_m \left(\frac{1 + r_m/\epsilon}{1 + r_m} - \frac{1 + r_d/\epsilon}{1 + r_d} \right) \left(\frac{1 + r_d}{1 + r_d/\epsilon} \right) : \tag{13}$$

Equation (13) is derived without approximations about the amount of water vapor and the amplitude of ΔT. Although this form is quite accurate, we would like to simplify it by assuming water vapor is a trace gas: $r \ll 1$. This is a good assumption for the current climate and may still be good till surface temperature reaches 320 K, at which temperature $r^*(p_s) = 73$ g/kg. With this approximation, we get

$$\Delta T_{WBG} = T_m \left(\frac{1}{\epsilon} - 1 \right) (r_m - r_d) : \tag{14}$$

This simplified equation clearly tells that ΔT depends on the contrast, not just absolute values, of mixing ratio and molar mass.

The above calculation is more accurate in the free troposphere, where gravity waves efficiently smooth out buoyancy anomalies. Although there is no such constraints in the boundary layer, we can assume that $\Delta T = 0$ at the surface temperature because of the uniform sea surface temperature (SST). We, therefore, require ΔT equals ΔT_{WBG} in the free troposphere but smoothly decays to 0 at surface:

$$\Delta T = \Delta T_{WBG} \times \left(1 - \frac{p}{p_s} \right)^n ; \tag{15}$$

where n controls the decay rate with pressure. The p/p_s term would decay faster (slower) with large (small) n, so different n could potentially result in different amplitudes and altitudes of the

maximum temperature difference. We, however, find that the values of ΔOLR and its sensitivity to surface temperature only change by 50% while we vary n over an order of magnitude, from 5 to 50. Therefore, we conclude the results are robust to the choice of n, and we take $n = 30$ in the following calculation. Figure 3a shows ΔT profiles at different surface temperatures. We find that the peak of ΔT is around 900 hPa, and that its peak is about 1.5 K at $T_s = 300$ and $b = 0.5$. We also find that ΔT increases faster with T_s in drier columns, which would be used to explain the sensitivity of ΔOLR to T_s.

Equations (5-9, 15) form the complete set of this model. With proper parameter values, we can estimate the magnitude of ΔOLR and its change with surface temperature.

f. Results

Our calculation shows that the vapor buoyancy effect can significantly impact Earth's energy balance and future climate changes. Figure 4a shows that ΔOLR is of $O(4\ \mathrm{W/m^2})$ for a wide range of parameter values. In the reference climate ($T_s = 300$ K), ΔOLR is about 2.5 W/m^2 with $b = 0.5$, a similar magnitude to the radiative effect due to doubling CO_2. According to (5), ΔOLR would increase with higher T, larger ΔT, or that the altitude of ΔT maximum becomes closer to the emission level, where $t \sim O(1)$. We use this principle to understand the sensitivity of ΔOLR to T_s and b.

- ΔOLR increases with T_s at given b. This is mainly because ΔT increase with warming, as will be quantified in Figs. 4b & 4c.

- ΔOLR is small at both moist and dry limits. In the moist limit ($b \to 1$), ΔT is small according to (14). In the dry limit ($b \to 0$), although ΔT maximizes, ΔOLR is dominated by surface emission, insensitive to ΔT. The OLR difference, therefore, peaks at intermediate b values.

- The ΔOLR peak shifts toward smaller b in warmer climates. This is because, at high temperatures, ΔT increases faster with warming in the small-b columns (Fig. 3a) and also because the large-b columns become increasingly opaque to IR emission (Fig. 3b-c).

Consistent with our hypothesis, ΔOLR increases with T_s, showing a negative climate feedback. To quantify the feedback strength, we define feedback parameters

$$l_t = \frac{d\Delta OLR}{dT_s}; \tag{16}$$

$$l_{vb} = \frac{d\Delta OLR}{dT_s}_{T;t}; \tag{17}$$

where l_t is the total sensitivity of ΔOLR to T_s, and l_{vb} is the vapor-buoyancy feedback parameter, which only concerns $d\Delta T$=dT_s. Figure 4b shows that l_t is of O(0.2 W/m^2/K) in the reference climate, which compares with the feedback strength due to clouds and surface albedo. The feedback parameter keeps increasing with surface temperature and reaches about 1.4 W/m^2/K at 320 K, suggesting that the vapor buoyancy effect becomes increasingly important in future climates.

Figure 4c shows that l_{vb} is of similar magnitude to l_t, suggesting the vapor-buoyancy feedback dominates the entire ΔOLR sensitivity to T_s. We find that l_{vb} is small at the moist and dry limits. This is because $\Delta T \to 0$ when $b \to 1$ at all surface temperatures, and ΔOLR is dominated by surface emission when $b \to 0$ at all surface temperatures, not feeling ΔT and its changes. In addition, we find that the peak of l_{vb} moves towards small-b columns with warming because ΔT increases faster with warming at small-b columns (Fig. 3a), and also because large-b columns become increasingly opaque at high temperature (Fig. 3b-c), insensitive to changes of ΔT that peaks in the lower troposphere.

The overall results do not depend on the assumed ΔT profiles in the boundary layer. Figure 4d-f shows ΔOLR, l_t, and l_{vb} for the free troposphere (p < 900 hPa). The free-troposphere results almost reproduce the full-column results, with amplitudes of 10 - 15% weaker than the full-column

calculation. This suggests that the vapor-buoyancy radiative effect and feedbacks occur primarily in the free troposphere.

4. Conclusion and discussion

The conventional wisdom is that the vapor buoyancy effect is small, so its impact on temperature is negligible in the free troposphere. However, using NASA AIRS observations, we have demonstrated that the vapor buoyancy effect could lead to about 1.5 K horizontal temperature difference in the lower troposphere, which has significant impact on Earth's radiative balance.

Based on the novel observation, this paper proposes that the vapor buoyancy effect can increase Earth's OLR by increasing air temperature in the dry columns. We have developed a simple model that computes the OLR difference between two atmospheres: one with the vapor buoyancy effect, and the other without this effect. We show that the magnitude of this effect is of $O(1\ \mathrm{W/m^2})$ at T_s = 300 K and that it increases rapidly with climate warming due to exponential increase of atmospheric water vapor, leading to a negative climate feedback (Fig. 2b). We further show that the feedback strength I is of $O(0.2\ \mathrm{W/m^2/K})$, the amplitude of which compares with major climate feedbacks, including cloud feedbacks and surface albedo feedbacks. Therefore, faithful representation of the vapor buoyancy effect in climate models is necessary for accurate estimates of climate sensitivity and reliable predictions for future climate changes.

The vapor buoyancy effect may help explain why tropical climate has been more stable than extratropical climate (Holland and Bitz 2003; Polyakov et al. 2002; Pierrehumbert 1995). The strength of the vapor buoyancy feedback depends on water vapor contrast between moist and dry columns, which in turn depends on water vapor abundance and thereby temperature in the atmosphere. This effect, therefore, operates more efficiently in the tropics and less efficiently at higher latitudes. This spatial pattern may explain why fluctuations of sea surface temperature in the

tropics are much smaller than that of higher latitudes in the past 100 million years (Pierrehumbert 1995).

The vapor buoyancy effect helps extend the inner edge of the habitable zone, in particular, for tidally locked exoplanets. Tidally locked planets are often slowly rotating, so their free troposphere could be in the WBG regime globally (Koll and Abbot 2016; Mills and Abbot 2013). These planets have one fixed diurnal hemisphere and one nocturnal hemisphere, corresponding to the moist and dry columns of our model, respectively. When the tidally locked planets are approaching the inner edge of the habitable zone, their surface temperature could be significantly higher than Earth's tropical SST, providing an ideal environment for the vapor buoyancy feedback to work efficiently. However, previous studies have neglected the vapor buoyancy effect and assumed WTG (Yang et al. 2013; Yang and Abbot 2014; Pierrehumbert 2010), which could lead to considerably narrower habitable zones. Therefore, we suggest that the vapor buoyancy effect should be accurately represented not only in GCMs but also in low-order models that are used to study climate habitability.

To focus on order-of-magnitude understanding, we have inevitably introduced simplifications to our model that only considers the clear-sky longwave radiation. An important one is that we use the two-band radiative transfer model, lacking detailed representation of water vapor's absorption spectrum. We have also assumed that b is uniform in altitude, whereas b often has complicated vertical structures in the real atmosphere. However, a suite of cloud-resolving model (CRM) simulations has shown similar estimates of $\mathsf{D}OLR$ and l. The CRM uses a comprehensive radiation scheme and explicitly simulates atmospheric circulations and water vapor dynamics. The CRM results have also shown that the vapor buoyancy effect does not affect the short-wave radiation budget and that the clear-sky effect dominates the OLR response. The CRM results, therefore, justify our simplifications and will be presented in a companion paper (Seidel and Yang 2018).

Acknowledgments.

References

Beucler, T., and T. W. Cronin, 2016: Moisture-radiative cooling instability. URL http://doi.wiley.com/10.1002/2016MS000763, 1620–1640 pp., doi:10.1002/2016MS000763.

Bretherton, C. S., P. N. Blossey, and M. Khairoutdinov, 2005: An Energy-Balance Analysis of Deep Convective Self-Aggregation above Uniform SST. *Journal of the Atmospheric Sciences*, **62 (12)**, 4273–4292, doi:10.1175/JAS3614.1.

Bretherton, C. S., and P. K. Smolarkiewicz, 1989: Gravity waves, compensating subsidence and detrainment around cumulus clouds. *Journal of the Atmospheric Sciences*, **46 (6)**, 740–759, doi:10.1175/1520-0469(1989)046⟨0740:GWCSAD⟩2.0.CO;2.

Charney, J. G., 1963: A Note on Large-Scale Motions in the Tropics. *Journal of the Atmospheric Sciences*, **20 (6)**, 607–609, doi:10.1175/1520-0469(1963)020⟨0607:ANOLSM⟩2.0.CO;2, URL http://journals.ametsoc.org/doi/abs/10.1175/1520-0469{\%}281963{\%}29020{\%}3C0607{\%}3AANOLSM{\%}3E2.0.CO{\%}3B2.

Collins, M., and Coauthors, 2013: Long-term Climate Change: Projections, Commitments and Irreversibility. In: Climate Change 2013: The Physical Science Basis. Contribution of Working Group I to the Fifth Assessment Report of the Intergovernmental Panel on Climate Change [Stocker, T.F., D. Qin, G.-K. Plattner, M. Tignor, S.K. Allen, J. Boschung, A. Nauels, Y. Xia, V. Bex and P.M. Midgley (eds.)]. Cambridge University Press, Cambridge, United Kingdom and New York, NY, USA.

Emanuel, K. A., 1994: Atmospheric convection. Oxford University press. 1994. pp. 580. isbn 0 19 5 6630 8.

Flato, G., and Coauthors, 2013: Evaluation of Climate Models. In: Climate Change 2013: The Physical Science Basis. Contribution of Working Group I to the Fifth Assessment Report of the Intergovernmental Panel on Climate Change [Stocker, T.F., D. Qin, G.-K. Plattner, M. Tignor, S.K. Allen, J. Boschung, A. Nauels, Y. Xia, V. Bex and P.M. Midgley (eds.)]. Cambridge University Press, Cambridge, United Kingdom and New York, NY, USA. doi: 10.1017/CBO9781107415324.020.

Held, I. M., and B. J. Soden, 2000: Water vapor feedback and global warming. *Annual Review of Energy and the Environment*, **25 (1)**, 441–475, doi:10.1146/annurev.energy.25.1.441, URL https://doi.org/10.1146/annurev.energy.25.1.441.

Holland, M. M., and C. M. Bitz, 2003: Polar amplification of climate change in coupled models. *Climate Dynamics*, **21 (3)**, 221–232, doi:10.1007/s00382-003-0332-6, URL https://doi.org/10.1007/s00382-003-0332-6.

Ingersoll, A. P., 1969: The runaway greenhouse: A history of water on venus. *Journal of the Atmospheric Sciences*, **26 (6)**, 1191–1198, doi:10.1175/1520-0469(1969)026⟨1191:TRGAHO⟩2.0.CO;2, URL https://doi.org/10.1175/1520-0469(1969)026⟨1191:TRGAHO⟩2.0.CO;2, https://doi.org/10.1175/1520-0469(1969)026⟨1191:TRGAHO⟩2.0.CO;2.

Koll, D. D. B., and D. S. Abbot, 2016: TEMPERATURE STRUCTURE AND ATMOSPHERIC CIRCULATION OF DRY TIDALLY LOCKED ROCKY EXOPLANETS. *The Astrophysical Journal*, **825 (2)**, 99, doi:10.3847/0004-637x/825/2/99, URL https://doi.org/10.3847%2F0004-637x%2F825%2F2%2F99.

Manabe, S., and R. T. Wetherald, 1967: Thermal equilibrium of the atmosphere with a given distribution of relative humidity. *Journal of the Atmospheric Sciences*, **24 (3)**,

241–259, doi:10.1175/1520-0469(1967)024⟨0241:TEOTAW⟩2.0.CO;2, URL https://doi.org/10.1175/1520-0469(1967)024⟨0241:TEOTAW⟩2.0.CO;2.

Manabe, S., and R. T. Wetherald, 1975: The effects of doubling the co2 concentration on the climate of a general circulation model. *Journal of the Atmospheric Sciences*, **32 (1)**, 3–15, doi:10.1175/1520-0469(1975)032⟨0003:TEODTC⟩2.0.CO;2, URL https://doi.org/10.1175/1520-0469(1975)032⟨0003:TEODTC⟩2.0.CO;2.

Mills, S. M., and D. S. Abbot, 2013: UTILITY OF THE WEAK TEMPERATURE GRADIENT APPROXIMATION FOR EARTH-LIKE TIDALLY LOCKED EXOPLANETS. *The Astrophysical Journal*, **774 (2)**, L17, doi:10.1088/2041-8205/774/2/l17, URL https://doi.org/10.1088%2F2041-8205%2F774%2F2%2Fl17.

Pierrehumbert, R. T., 1995: Thermostats, radiator fins, and the local runaway greenhouse. *Journal of the Atmospheric Sciences*, **52 (10)**, 1784–1806, doi:10.1175/1520-0469(1995)052⟨1784:TRFATL⟩2.0.CO;2, URL https://doi.org/10.1175/1520-0469(1995)052⟨1784:TRFATL⟩2.0.CO;2, https://doi.org/10.1175/1520-0469(1995)052⟨1784:TRFATL⟩2.0.CO;2.

Pierrehumbert, R. T., 2010: A PALETTE OF CLIMATES FOR GLIESE 581g. *The Astrophysical Journal*, **726 (1)**, L8, doi:10.1088/2041-8205/726/1/l8, URL https://doi.org/10.1088%2F2041-8205%2F726%2F1%2Fl8.

Pierrehumbert, R. T., 2010: *Principles of Planetary Climate*.

Polyakov, I. V., and Coauthors, 2002: Observationally based assessment of polar amplification of global warming. *Geophysical Research Letters*, **29 (18)**, 25–1–25–4, doi:10.1029/2001GL011111, URL https://agupubs.onlinelibrary.wiley.com/doi/abs/10.1029/2001GL011111, https://agupubs.onlinelibrary.wiley.com/doi/pdf/10.1029/2001GL011111.

Pritchard, M. S., and D. Yang, 2016: Response of the superparameterized Madden-Julian Oscillation to extreme climate and basic state variation challenges a moisture mode view. *Journal of Climate*, JCLI–D–15–0790.1, doi:10.1175/JCLI-D-15-0790.1, URL http://journals.ametsoc.org/doi/abs/10.1175/JCLI-D-15-0790.1.

Seidel, S., and D. Yang, 2018: The virtual effect of water vapor helps stabilize tropical climate. *AGU Fall Meeting*, URL https://agu.confex.com/agu/fm18/meetingapp.cgi/Paper/423217.

Sobel, A. H., J. Nilsson, and L. M. Polvani, 2001: The Weak Temperature Gradient Approximation and Balanced Tropical Moisture Waves*. *Journal of the Atmospheric Sciences*, **58 (23)**, 3650–3665, doi:10.1175/1520-0469(2001)058⟨3650:TWTGAA⟩2.0.CO;2.

Tompkins, A. M., 2001: Organization of Tropical Convection in Low Vertical Wind Shears: The Role of Water Vapor. *Journal of the Atmospheric Sciences*, **58 (6)**, 529–545, doi:10.1175/1520-0469(2001)058⟨0529:OOTCIL⟩2.0.CO;2, URL http://journals.ametsoc.org/doi/abs/10.1175/1520-0469(2001)058{\%}3C0529:OOTCIL{\%}3E2.0.CO;2.

Yang, D., 2018a: Boundary layer diabatic processes, the virtual effect, and convective self-aggregation. *Journal of Advances in Modeling Earth Systems*, **10 (9)**, 2163–2176, doi:10.1029/2017MS001261, URL https://agupubs.onlinelibrary.wiley.com/doi/abs/10.1029/2017MS001261, https://agupubs.onlinelibrary.wiley.com/doi/pdf/10.1029/2017MS001261.

Yang, D., 2018b: Boundary layer height and buoyancy determine the horizontal scale of convective self-aggregation. *Journal of the Atmospheric Sciences*, **75 (2)**, 469–478, doi:10.1175/JAS-D-17-0150.1, URL https://doi.org/10.1175/JAS-D-17-0150.1, https://doi.org/10.1175/JAS-D-17-0150.1.

Yang, D., and A. P. Ingersoll, 2013: Triggered Convection, Gravity Waves, and the MJO: A Shallow-Water Model. *Journal of the Atmospheric Sciences*, **70 (8)**, 2476–2486, doi:10.1175/JAS-D-12-0255.1, URL http://dx.doi.org/10.1175/JAS-D-12-0255.1.

Yang, D., and A. P. Ingersoll, 2014: A theory of the MJO horizontal scale. *Geophysical Research Letters*, 661–666, doi:10.1002/2013GL058542, URL http://onlinelibrary.wiley.com/doi/10.1002/2013GL058542/epdf.

Yang, J., and D. S. Abbot, 2014: A LOW-ORDER MODEL OF WATER VAPOR, CLOUDS, AND THERMAL EMISSION FOR TIDALLY LOCKED TERRESTRIAL PLANETS. *The Astrophysical Journal*, **784 (2)**, 155, doi:10.1088/0004-637x/784/2/155, URL https://doi.org/10.1088%2F0004-637x%2F784%2F2%2F155.

Yang, J., N. B. Cowan, and D. S. Abbot, 2013: STABILIZING CLOUD FEEDBACK DRAMATICALLY EXPANDS THE HABITABLE ZONE OF TIDALLY LOCKED PLANETS. *The Astrophysical Journal*, **771 (2)**, L45, doi:10.1088/2041-8205/771/2/l45, URL https://doi.org/10.1088%2F2041-8205%2F771%2F2%2Fl45.

LIST OF FIGURES

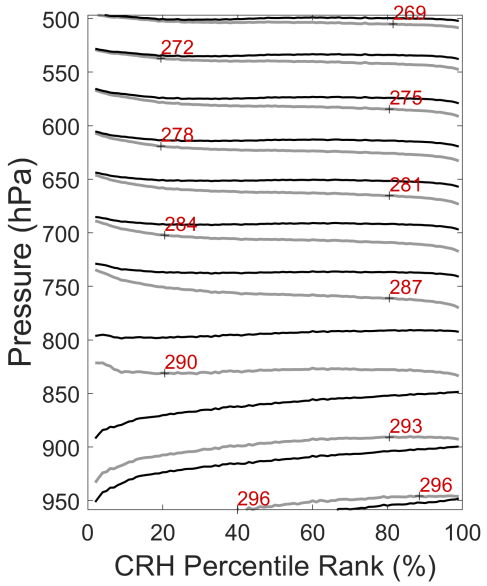

FIG. 1. Temperature and virtual temperature fields in the moisture space using NASA AIRS data from 2^oS to 2^oN for the calendar year 2017. Black contours correspond to virtual temperature, and gray contours correspond to temperature. The x-axis is column relative humidity (CRH) rank, where CRH was calculated as precipitable water divided by saturation precipitable water above the altitude of 850 hPa. The driest columns are to the left, and the moistest columns are to the right. The temperature contours are tilted due to the vapor buoyancy effect.

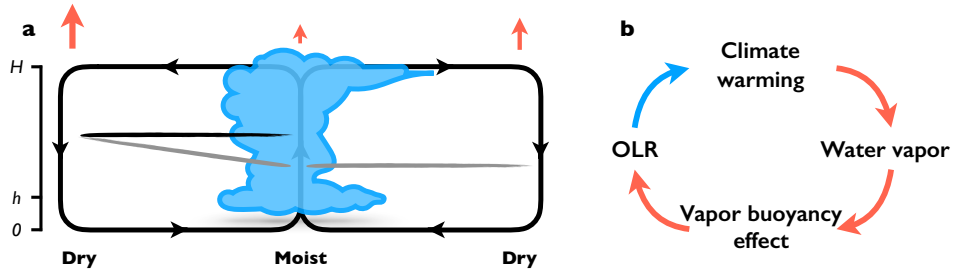

FIG. 2. Schematic diagrams. **a)** The vapor buoyancy effect increases OLR in the tropical atmosphere. This figure depicts two stand-alone atmospheres: the control atmosphere (left); no-vapor-buoyancy atmosphere (right). The horizontal axis is x or CRH; the vertical axis is height (h = boundary layer height, H = tropopause height). The gray lines represent temperature contours, and the black line represent buoyancy or virtual temperature contour. The orange arrows represent OLR emission: large (small) arrow corresponds to more (less) OLR. **b)** The negative climate feedback. Orange arrows represent an increase effect; the blue arrow represents a decrease effect.

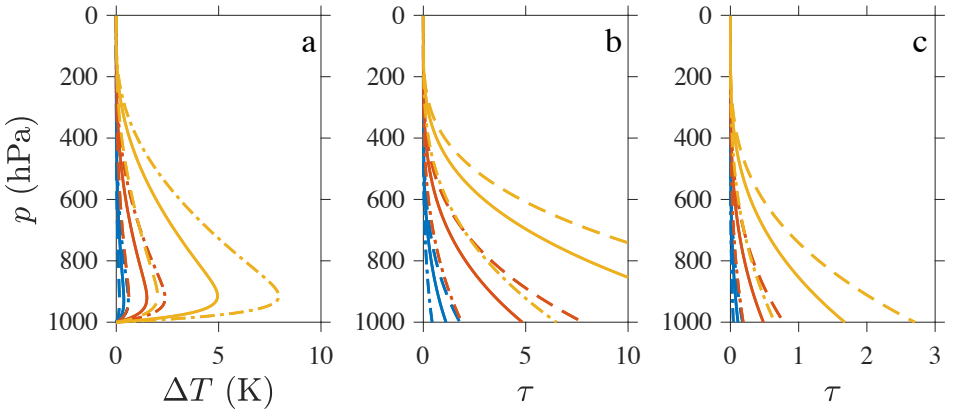

FIG. 3. (a) DT profiles (K). (b) t profiles for the strong absorption band. (c) t profiles for the weak absorption band. Blue: 280 K, red: 300 K, yellow: 320 K. Dot-dashed: b = 0:2; solid: b = 0:5; dashed: b = 0:8.

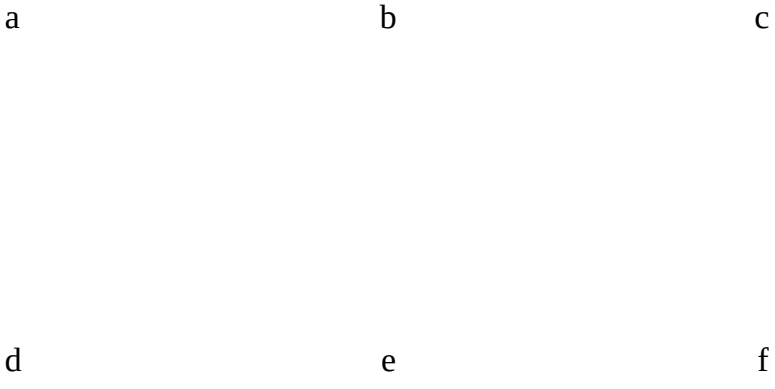

436 FIG. 4. (a) The radiative effect D*OLR* (W/m^2) due to the vapor buoyancy effect. The blue curve corresponds
437 to D*OLR* = 1 W/m^2. (b) The total feedback parameter l_t (W/m^2/K). (c) The feedback parameter l_{vb} (W/m^2/K)
438 of the vapor buoyancy feedback. The blue curve corresponds to l = 0.1 W/m^2/K in (b-c). (d-f) D*OLR*, l_t, and
439 l_{vb} for the free troposphere (p < 900 hPa), respectively.